

Fatigue of steel bridges

U. Kuhlmann^{a*}, S. Bove^a, S. Breunig^a and K. Drebenstedt^a

^aInstitute of Structural Design, University of Stuttgart, Germany

*corresponding author, e-mail address: sekretariat@ke.uni-stuttgart.de

Abstract

Highway and railway bridges are exposed to cyclic stressing due to traffic loads and, therefore, have to be evaluated concerning fatigue. In most cases the fatigue evaluation is performed according to Eurocode 3 Part 1-9 on nominal stresses. To apply this nominal stress approach a detail catalogue is required classifying all relevant constructional details in terms of fatigue. Unfortunately, the existing detail catalogue of Eurocode 3 Part 1-9 reflects the state of the art of the 1990s and misses constructional details being important for today's bridge design. As an example the derivation of a new detail, the so-called lamellae joint, is presented. Furthermore, for two new types of innovative steel bridges, where Eurocode 3 Part 1-9 does not yet specify rules able to evaluate the characteristics of these bridges, research results are shown. These are the thick-plate trough bridges and truss bridges made of thick-walled circular hollow sections (CHS). The paper starts with an overview on the recent Eurocode developments, addressing more specific the fatigue verification according to EN 1993-1-9 and the statistical analysis of fatigue test data. In the following, information is given on the outcome of some recent research projects striving to extend the application range of Eurocode 3 Part 1-9. The final conclusion, in spite of all differences, show a common tendency.

Keywords: Fatigue; Steel bridges; Eurocode 3 Part 1-9; Statistical analysis; Lamellae joint; Circular hollow section trusses; Thick-plate trough bridges.

1. Introduction

Highway and railway bridges are exposed to cyclic stressing due to high traffic loads and, therefore, have to be evaluated concerning fatigue. In most cases the fatigue evaluation can be performed according to EN 1993-1-9 [1] on nominal stresses. To apply this nominal stress approach the detail catalogue, given by the Tables 8.1 to 8.10 in Eurocode 3 Part 1-9 and classifying a large spectrum of constructional details in terms of fatigue, has to be used. Unfortunately, this detail catalogue reflects the state of

the art of the 1990s and misses constructional details being important for today's bridge.

As an example, the top or bottom flanges of steel and composite bridges consist in many cases of more than one plate welded on top of one another. In order to connect such stacks of steel plates on site, a so-called lamellae joint as visualized in Fig. 1 (c), can be used. However, this detail is not part of the basic standards like [1] or [2] and is not mentioned in the recommendations of the *International Institute of Welding*

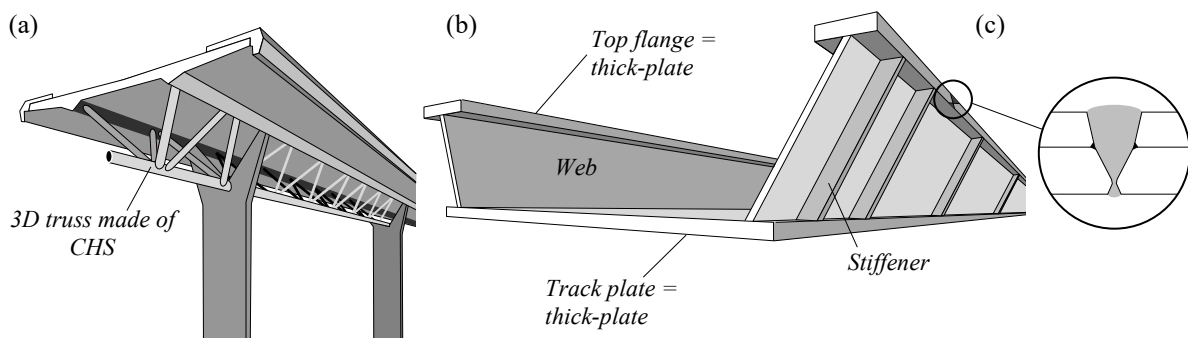


Fig. 1. (a) Example of a steel-concrete composite highway bridge, taken from [3], (b) example of a thick-plate trough bridge and (c) an example of a typical lamellae joint.

(IIV) [4]. As being built in practice, this detail is addressed in this paper based on recent research.

Thick-plate trough bridges represent another example of a structure not totally covered by the existing design rules, as some constructional details are subjected to a complex stress state which leads to a difficult identification of design relevant stresses, see Fig. 1 (b).

Furthermore, Eurocode 3 Part 1-9 does not specify rules for bridge structures not able to be evaluated by the nominal stress approach. An example of such structures are welded circular hollow section (CHS) joints with thick-walled chords (Fig. 1 (a)), as the Eurocode covers only two-dimensional K-joint geometries with wall thicknesses t_0 and $t_1 \leq 8$ mm. In addition, the design rules of CIDECT [5] and DNV [6] limit the chord slenderness to

$$\gamma = d_0 / (2 \cdot t_0) \geq 12 \text{ and } 8 \quad (1)$$

respectively, where d_0 is the chord diameter and t_0 is the chord wall thickness.

For this purpose this paper is firstly going to focus on the current state of standardization, especially of the Eurocode 3 Part 1-9, in order to give a short overview of the current work under coordination of the European Committee for Standardization (CEN). Subsequently, the statistical analysis of fatigue test data is addressed, as a statistical evaluation constitutes the key for the derivation of fatigue strengths. In a further step, the outcome of some recent German research projects striving to extend the application range of Eurocode 3 Part 1-9 is presented.

2. State of standardization – Eurocode 3 Part 1-9

The Eurocodes have become the primary standards for structural and geotechnical design in Europe. An overview for the planned revision of the Eurocodes is given in Fig. 2. At the moment the 2nd Generation of Eurocodes is under preparation. All existing Structural Eurocodes including EC 3: Design of steel structure - Part 1-9: Fatigue will be further developed under coordination by the European Committee for Standardization (CEN) [7].

The revision of the Eurocodes comprises two phases. The first part focuses on general revision and maintenance of the Eurocodes. The code revision is launched in form of a call for ‘system-

atic reviews’ to the national standardizing bodies. The suggestions and comments that are given in the systematic review will be evaluated and incorporated by CEN Subcommittees and Working Groups. The second main activity in the frame of the Eurocode revision cares about further evolution with focuses on new methods, new materials and new regulatory and market requirements. It is realized in the frame of the mandate M/515 [8], which was agreed in December 2012 between the European Commission and CEN. The final realization is conducted by so called Project Teams (PT) that consist of a maximum of six experts [8].

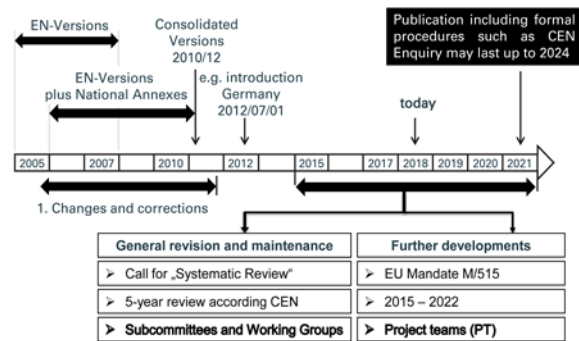


Fig. 2. Planned time-table for the revision of the Eurocodes.

The revision of EN 1993 Part 1-9 focuses mainly on a more user-friendly formulation and improved wording of the existing design rules. The practical application on Eurocode 3 Part 1-9 since 2005 and the systematic review of the standard in 2017 has identified a couple of unclear or ambiguous rules that require technical clarification. For example, the requirements on the fabrication in the fatigue detail catalogue in Sec. 8 of [1] are formulated too unclear and leave room for interpretation. A revision of the tables aims to clarify the figures and descriptions of the constructional details. The requirements on the fabrication of welded details will be clarified with help of an additional column that shows weld symbols. An example is given in Fig. 3. It shows a butt weld that is stressed in longitudinal direction. The symbol shows that a root backing is needed. Information regarding the fabrication of a fatigue loaded constructional detail are important, because their influence could be significant for the fatigue strength.

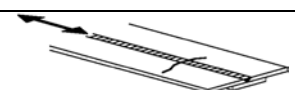

Detail category	Constructional detail	Symbol
100		

Fig. 3. Additional weld symbols.

In future the fatigue detail catalogue in EN 1993-1-9 will be complemented by new constructional details, which are required in practice. For example, the lamellae joint will be introduced, see Chapter 4.

3. Statistical Analysis of Fatigue Test Data

3.1. Background

The core of Eurocode 3 Part 1-9 is the fatigue assessment by using the corresponding fatigue detail category that is defined in the standard. The detail category defines the underlying $S-N$ curve, which is characterized by the reference value, $\Delta\sigma_C$, and the slope, m , of the $S-N$ curve. The curves are based on experimental data. In order to guarantee a uniform safety level, the fatigue strength of Eurocode 3 expressed by its characteristic reference value $\Delta\sigma_C$ for $2 \cdot 10^6$ stress cycles should be derived on the basis of standardized and commonly agreed criteria. Because of its scatter, there is a need for statistical analysis of the test data to define reliable values $\Delta\sigma_C$. However, in practice the values $\Delta\sigma_C$ are derived in different ways, which limit their comparability [9].

3.2. Regression Analysis

Generally, test data in the high cycle fatigue range (finite life) are allocated to a curve defining a linear relationship between the numbers of stress cycles to failure, N , and the applied stress ranges, S , according to *Basquin* [10] on a log-log scale using the least-square method. A so obtained $S-N$ curve defines the 50%-survival probability of the considered sample and has to be transformed into a characteristic $S-N$ curve for design purposes by statistical analysis.

In the frame of fatigue testing the stress level S is normally predetermined, therefore it is an independent variable. Contrarily, the number of stress cycles to failure N are dependent (on the stress level). According to *Basquin* [10] there is a linear relationship between $\log S$ and $\log N$ with decimal logarithm (base 10), see Eq. (2).

$$\log N = \log a - m \cdot \log S \quad (2)$$

where $\log N =$ logarithm (base 10) of corresponding number of cycles to failure N ; $\log a =$ intercept on the $\log N$ axis; $m =$ negative inverse of the mathematical slope of $S-N$ curve; $\log S =$ logarithm (base 10) of allowable stress range S .

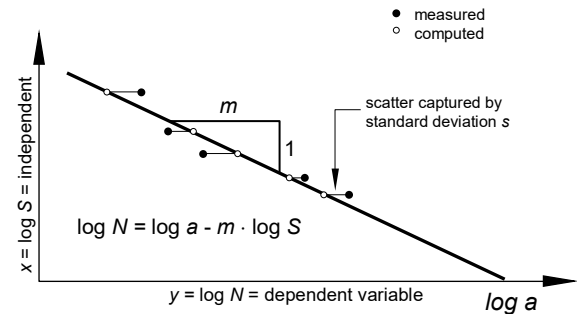


Fig. 4. Linear regression of $S-N$ curve.

Due to the scatter, there is a statistical uncertainty in the variables $\log a$ and m . These unknown model parameters are estimated from the fatigue data. If the slope of the $S-N$ curve is already known due to existing information, only $\log a$ has to be determined. The result forms an average $S-N$ curve representing the 50 % survival probability of the tested data set or rather of the sample, see Fig. 4.

3.3. Statistical Evaluation

There is a tendency for errors that occur in many real situations to be normally distributed. The normal distribution is also referred to as the Gaussian distribution. It can be shown graphically by a typical Gaussian bell curve, see Fig. 5.

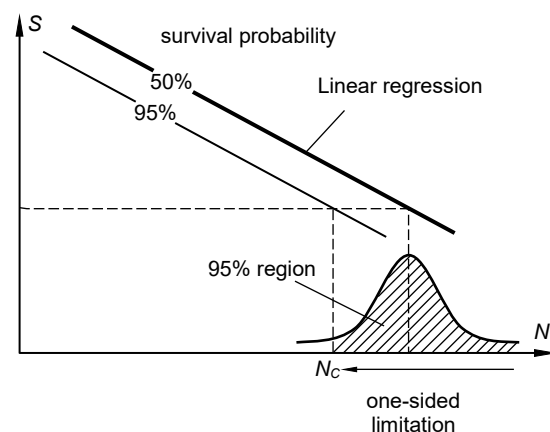


Fig. 5. Gaussian bell curve with one-sided limitation.

The normal distribution is defined by only two parameters: mean value and standard deviation, s . Is the sample sufficiently large to represent the whole population, the characteristic $S-N$ curve

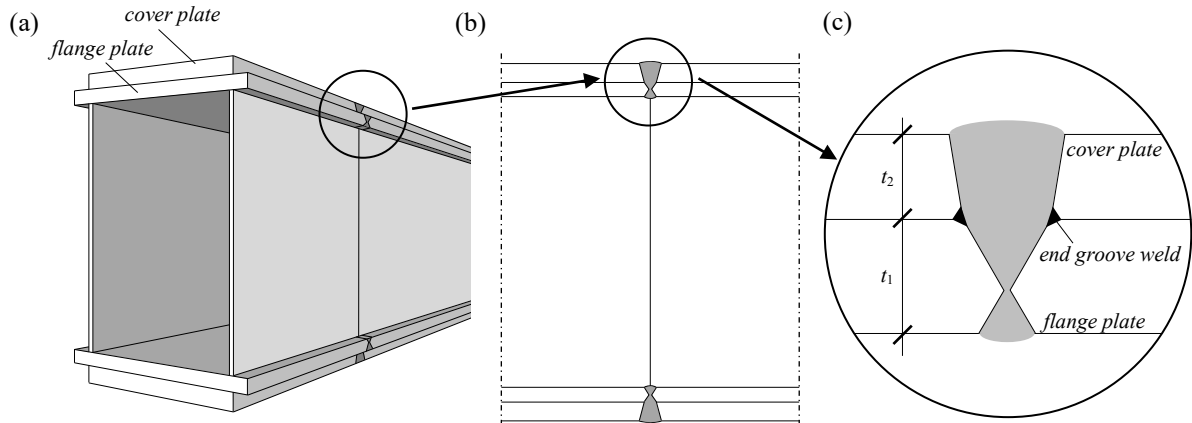


Fig. 6. Welding detail lamellae joint: (a) and (b) overview, (c) detail.

with 95 % probability of survival could be calculated with help of the corresponding fractile value of the normal distribution. EN 1990 [11] recommends at least 100 specimens to represent the whole population. Otherwise the statistical uncertainty associated with the number of tests should be taken into account. The so called prediction interval is an appropriate method to do so. A prediction interval is an estimate of an interval, in which m future observations are expected to fall in with a certain probability. It defines on the basis of the sample and under consideration of the statistical uncertainty, information about the scatter of fatigue resistance for a future structure. The prediction interval is using the t -distribution instead of the Gaussian distribution. It is defined by an additional third parameter: the degree of freedom. It takes into account the sample size and the amount of parameters with a statistical uncertainty. In case the degree of freedom becomes large, the shape of the distribution fits to the Gaussian bell curve. The coefficient t of Student's t distribution is tabulated in common literature, for example by *Wadsworth* [12].

Another possibility for statistical analysis is given in the Eurocode 0 [11]. The standard defines, among others, rules for design that is assisted by testing. The corresponding chapter in Eurocode 0, Annex D gives information about statistical determination. In case that there is only one parameter that is afflicted with a statistical uncertainty, Eurocode 0 and the prediction interval are giving identical results [9].

3.4. Summary

The derivation of a characteristic $S-N$ curve should take into account the scatter of test data,

statistical uncertainty associated with the number of tests and prior statistical knowledge. The prediction interval delivers a closed mathematical solution that is suitable for application in the frame of statistical analysis of fatigue data for constructional details in steel construction.

4. Introduction of a new constructional detail: the lamellae joint

4.1. Background

Plated steel girders are quite common in steel and composite bridge design. In consideration of the economic aspects, it is useful to vary the cross sections of the flanges by cover plates. The adaption of the flanges to the internal forces can be put into practice in two different ways. Either by using flanges with varying thickness or by using cover plates (lamellae) which are welded to the flange plate.

Due to restricted transport length and assembly weight, it is commonly necessary to implement in-situ joints in the girder that are called lamellae joints. In contrast to a common butt joint, the so-called end groove weld is characteristic for the lamellae joint and influences the joint's fatigue behavior, see Fig. 6.

The lamellae joint has been an important constructional detail in German bridge design since 1935. Therefore, in old German regulations such as DS 804 [13] and TGL 16500 [14] the lamellae joint was part of the fatigue detail catalogue. However, up to now the lamellae joint is missing in the fatigue detail catalogue of Eurocode 3 Part 1-9 [1].

4.2. Experimental investigations

A research project (DAST/IGF No. 15380) [15] realized by University of Stuttgart, Institute of Structural Design, investigated the size effect of the fatigue behavior of lamellae joints in detail including experimental investigations. Lamellae joints comprising two plates, according to Fig. 6 were tested. One primary goal of the research project was to identify whether the size effect depends on the maximum plate thickness of single plates connected by the lamellae joint or on the overall thickness of the joint.

In the follow-on research project (DAST/IGF No. 17104) [16] a larger range of parameters was investigated in an extensive test program.

There were four different test series. The plate thickness in these series included the application range common for bridge design. In test series No. 100 a pronounced size effect was expected. In contrast, it was expected that there is no size effect in test series No. 200 because of the thin single plates. The plate thickness of test series No. 300 was chosen between the two other series. The plate thickness ratio of the test series No. 100, 200 and 300 amounts to 0.8. To investigate the influence of a different plate thickness ratio, an additional test series No. 400 was carried out having a ratio of 0.5. Table 1 gives an overview of the test series.

Table 1. Fatigue tests on lamellae joints, from [15] and [16].

Objective	Size effect			Plate thickness ratio
	100	200	300	400
Test-series	100	200	300	400
t_1 [mm]	80	20	40	25
t_2 [mm]	100	25	50	50
t_1 / t_2	0.8	0.8	0.8	0.5
No. of specimens	15	10	15	10

4.3. Test results

The fatigue strength is directly linked with the stress concentration of the critical notches of the constructional detail's geometry. The investigations have shown three different types of critical notches, see Fig. 7.

- **Notch #1:** weld toe from surface layer of the thinner plate (t_1)
- **Notch #2:** weld toe from surface layer of the thicker plate (t_2)
- **Notch #3:** root run of the end groove weld

As observed during the fatigue tests, there are three potential modes of failure of the lamellae joint. The modes differ by various crack initiation points. The cracks can start at the weld toe (notch #1 or #2), but a crack initiation at the end groove weld (notch #3) is also possible.

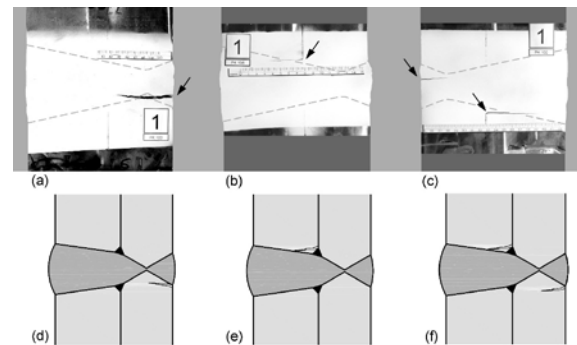


Fig. 7. Failure of the specimens No. (a) 103, (b) 106, (c) 102; (d) Crack starting from weld toe, (e) Crack starting from the end groove weld, (f) mixed crack mode.

Fig. 8 shows the failure of specimen No.109 with crack initiation at the weld toe.

Investigations on cracked specimens have shown that a discontinuity in the end groove weld is not necessarily an initiation point for the fatigue crack. Thus, the test results imply common irregularities in the root of weld.

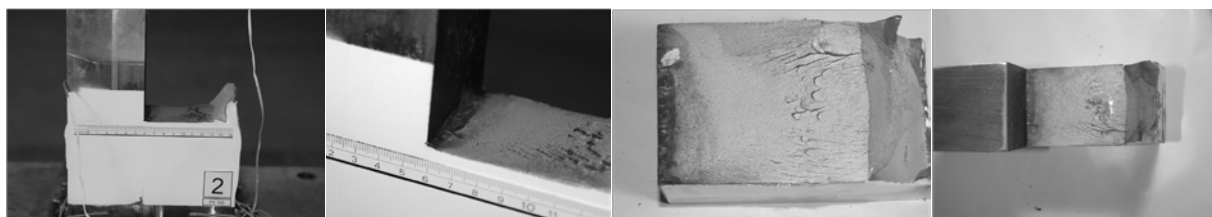


Fig. 8. Failure of the specimens.

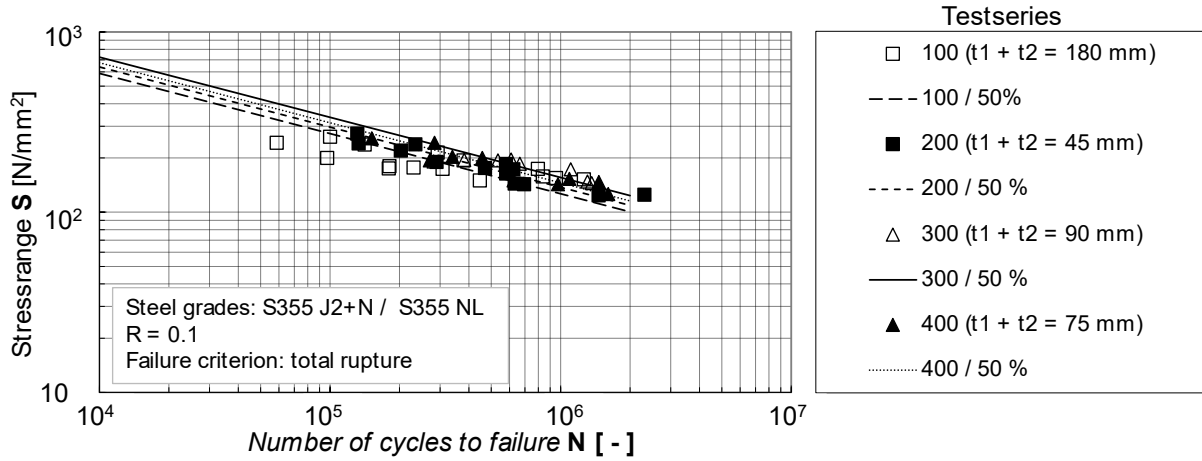


Fig. 9. Test results with 50 % S-N curves.

4.4. Statistical evaluation of test results

First, the series were evaluated individually by a linear regression analysis, see Fig. 9. A constant value of $m = 3$ has been assumed. Comparing the results of the different series in Fig. 9 it turns out, that the results of series 100 with high overall thickness of 180 mm are below the other results. This indicates that the fatigue strength of the specimens depends on the overall joint thickness.

According to Eurocode 3 Part-1-9 the size effect due to thickness should be taken into account as given in Eq. (3):

$$\Delta\sigma_{C,red} = k_s \cdot \Delta\sigma_C \quad (3)$$

where $\Delta\sigma_{C,red}$ is the reduced reference value of the fatigue strength; k_s is the reduction factor for fatigue stress to account for size effect; $\Delta\sigma_C$ is the reference value of the fatigue strength at $N_c = 2$ million cycles.

For plate packages with $t > 25$ mm the reduction factor is calculated as given in Eq. (4):

$$k_s = \left(\frac{25}{t}\right)^n \quad (4)$$

where t is the overall thickness of all plates and n is the correction exponent. The correction exponent n , could be determined on experimental basis by searching for the lowest standard deviation s , of the scatter.

For a conservative estimate, the value is set to $n = 0.2$. This is equal to the value for the thickness correction exponent for butt joints in Eurocode 3 Part 1-9.

Fig. 10 shows the nominal stress range transferred to 2 million cycles and scaled to reference thickness $t_{ref} = 25$ mm. The detail category of the overall statistical evaluation, based on the prediction interval, indicates a detail category 104. Nevertheless, it is proposed to apply detail category 90 for the constructional detail of the lamellae joint in the frame of Eurocode design. This detail category is equal to detail ⑤ in Eurocode 3 Part 1-9, Table 8.3: Transverse butt welds. Fig. 11 shows a proposal to apply the constructional

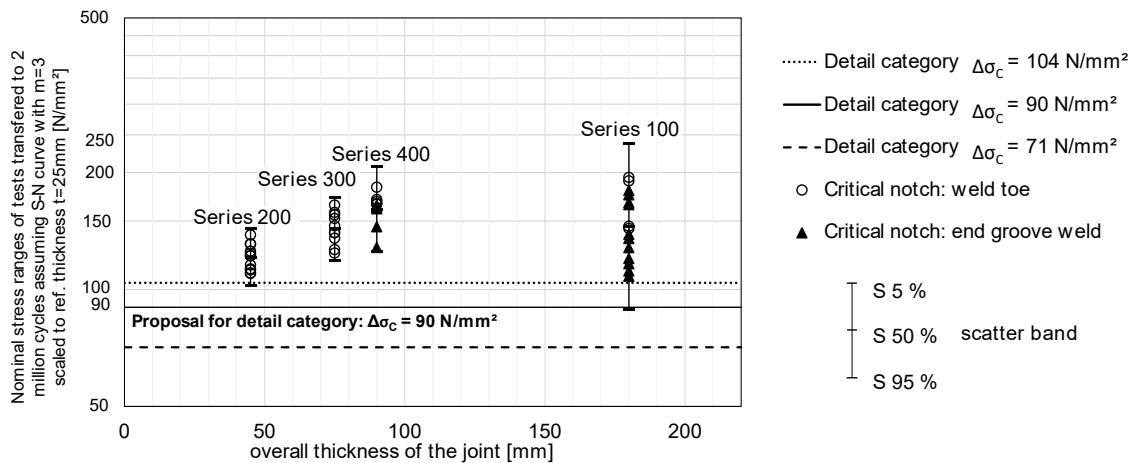


Fig. 10. Test results: proposal for detail category.

detail of the lamellae joint in the frame of Euro-code design, [17].

Detail category	Constructional detail	Symbol	Description	Requirements
90 size effect for $t > 25$ mm: $k_s = (25/t)^{0.2}$	<p>end groove weld</p>		Multiple plates, transverse butt weld	<ul style="list-style-type: none"> - See detail ⑤, ⑥, ⑦. - When the butt joint is welded, the end groove weld should not melt. - The root of the butt weld should be positioned in the center of the cover- or flange plate

Fig. 11. Proposed change: additional row in Table 8.3: transverse butt weld.

5. Developments and fatigue behavior of short span railway steel bridges as thick-plate trough bridge

5.1. Introduction

One promising steel bridge solution for railway bridges of small spans is the thick-plate trough bridge. The steady improvement of fabrication processes and welding properties in the steel plate production led to an innovative design of cross sections for short span railway bridges. With steel plates of thicknesses from around 80 to 120 mm, the so-called thick-plate trough bridges came up around 20 to 25 years ago.

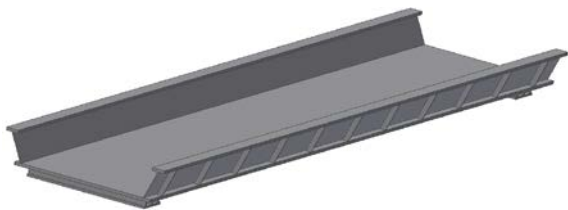


Fig. 12. Isometric view of thick-plate trough bridge [18].

An isometric illustration of the thick-plate trough bridge is given in Fig. 1(b) and Fig. 12, clearly showing the improvement in construction height because no transverse girders are necessary. In order to save thick-plate material the webs are not perpendicular, but declined fillet welded to the bottom plate.

This type of construction is especially interesting for the replacement of railway constructions in inner city areas, where a change of the

rail track is restricted especially in height because of the conditions of the existing structure. Another advantage is the simple erection due to the possibility to prefabricate the whole steel superstructure and erect it by crane lifting in one piece.

5.2. Project overview and motivation

In the frame of the German cooperative FOSTA-AiF research project called ‘Holistic Assessment of Steel- and Composite Railway Bridges according to Criteria of Sustainability’ [18], three different railway bridge types were evaluated in terms of sustainability. Therefore, three typical bridges for different application fields were chosen and were compared to variants in view of economical, ecological and socio-functional aspects, see [18] and [19].

Among the three bridge types, the thick-plate trough bridge was chosen as steel bridge solution for railway bridges of small spans. When it comes to the economical, ecological and socio-functional assessment of a bridge, the durability of the construction plays an important role. The durability of a steel bridge construction and thus its sustainability is mainly affected by corrosion processes and fatigue phenomena. Especially for heavy loaded railway bridges the fatigue assessment is defining the design.

Within the project [18], the thick-plate trough bridge was investigated in terms of construction and design, especially regarding the fatigue behavior. In the following, the latest findings of [18] and [20] concerning the fatigue behavior of thick-plate trough bridges are summarized.

5.3. Load distribution

For this type of bridge, the thick-plate deck unifies the function of the bottom flange of the main girder as well as the track plate. Transverse girders become dispensable, as the up to 100 mm thick plate transfers the direct loading to the main girders. This effect, which can be seen in Fig. 13, leads to a large deflection of the bottom plate in vertical direction, with a maximum in the center of the bridge, under load model 71 (LM71), the nominal load model for normal railway tracks according to EN 1991-2 [21].

As a consequence of the clamping of the web to the stiff thick-plate, a bending moment occurs

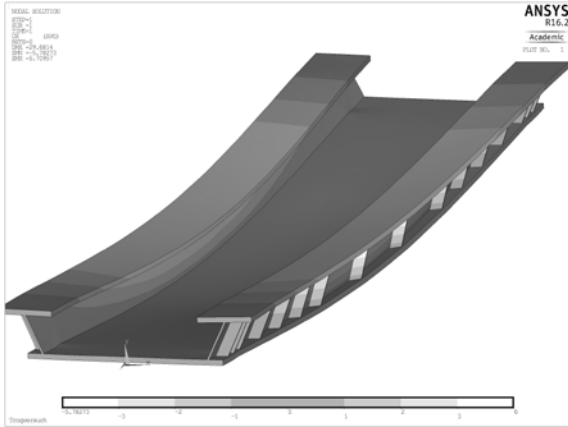


Fig. 13. Sum of deformations of thick-plate trough bridge [20].

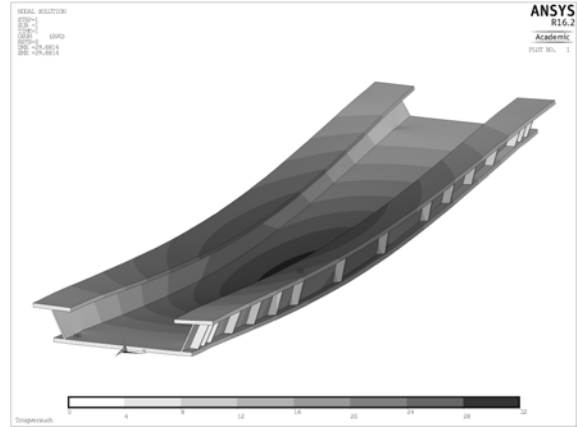


Fig. 14. Horizontal deformations of thick-plate trough bridge [20].

around the thickness of the web. This transversal bending of the web has to be transferred by the double fillet welds connecting the web to the bottom thick-plate. This is illustrated in Fig. 14, where the horizontal deformations of the trough bridge as a result of LM71 loading is given.

Therefore, the double fillet weld is loaded by direct stresses from the global bending moment respectively the resulting shear action of the bending moment of the main girder as well as this transversal bending moment resulting from the transverse frame action of web and thick plate.

Fig. 14 gives the horizontal deformations in an elastic FE-Analysis, clearly showing that the upper flanges with the webs tend to come to the middle of the bridge.

The effect of transversal bending even increases for the T-section, where the main girder is supported by a transverse stiffener. This transversal bending of the fillet weld is mostly neglected in the design process. Lateral torsional buckling of the main girders is prevented by a

high number of transverse stiffeners, supporting the webs and connected to the upper flanges of the main girders and the bottom thick-plate.

Following the aim of [18] to improve this bridge structure, save fabrication costs and maintenance time and costs, the number of transverse stiffeners may be reduced, however the effects of transversal bending would be increased.

Previous investigations from *Schrade* [22] on different thick-plate bridges have shown that the deflection of this bridge type can be estimated with the help of the analytical method of the Generalized Beam Theory, also see [23]. Since this method is applicable for prismatic cross sections considering the distortion of the cross-section, the results revealed that there is a significant bending moment at the location of the connection of the double fillet welds between web and thick-plate. Especially, when it comes to the fatigue assessment this welded connection represents a sharp notch.

This is why *Schrade* [22] recommends butt welds instead of fillet welds connecting the web

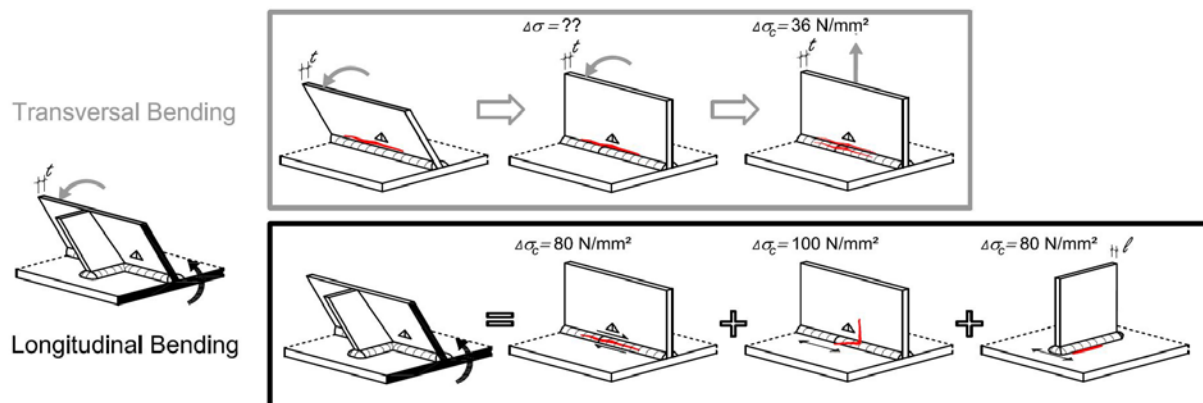


Fig. 15. Categorisation of longitudinal bending and transversal bending from [20] in weld detail categories of EN 1993-1-9.

to the upper and the bottom flange. Furthermore, in [22] a web plate thickness of 40 mm is recommended, whereas the common practice is a web plate thickness of 30 mm. So the question arises if this transversal bending at the connection is purely theoretical and minimal or real and measurable, and thus may be decisive.

5.4. Fatigue behavior

When it comes to the fatigue design according to EN 1993-2 [2] and EN 1993-1-9 [1], using the nominal stress approach, several fatigue details have to be considered individually to enable the comparison with the detail categories given in the tables in EN 1993-1-9.

Therefore, a consideration according to the directions of internal forces can be useful. As can be seen from Fig. 15, where a half of the main girder with a transverse stiffener is cut out, there is longitudinal bending and transversal bending for two different “T-sections”. Trying to assess these details due to the existing fatigue details according to EN 1993-1-9 [1] one has to further differentiate.

Identifying the single welded details according to the detail catalogue in EN 1993-1-9 one question occurs: for transversal bending of a double fillet weld, no detail category exists. Thus, to cover this effect on the safe side, the detail of the tensioned T-stub with fillet welds (see Table 8.5 Detail 3, in [1]) is usually chosen, which is the lowest detail category in EN 1993-1-9 with a fatigue resistance of only 36 N/mm².

In addition, the constructional details of the transverse stiffener welded to the bottom thick-plate, see Fig. 15, and the longitudinal fillet weld under shear welded to the tension flange (the thick-plate), see Fig. 15, have to be considered.

The complex stress state at the bottom plate in combination with the accumulation of welded details and the additional effects of transversal bending led to the necessity of experimental and numerical investigations for the fatigue design of this innovative type of trough bridge.

5.5. Test results on double fillet welds under web plate bending

Within two series of small scale tests with differing plate thicknesses (series 100 and series 200) the fatigue resistance of the transversally bended longitudinal fillet welds could be investigated, see Fig. 16. By using a configuration of

a thick-plate of 100 mm and a web plate thicknesses of 30 mm (Series 200) a significant scale effect was detected, compared to Series 100 with 30 mm track plate dimension and 10 mm web plate thickness.

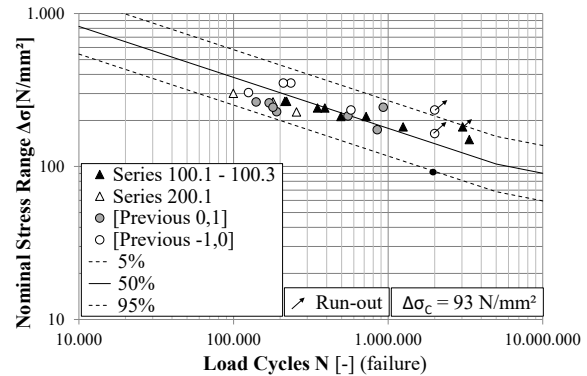


Fig. 16. Results of small scale tests under transversal plate bending (with size effect correction).

Previous fatigue test results from investigations on slender bridge webs from *Guenther et al.* [24] and bended crane girder webs of *Kuhlmann et al.* [25] could be used in addition to the current results to determine a fatigue resistance for transversally bended fillet welds. The evaluation leads to a fatigue resistance $\Delta\sigma_c$ of around 90 N/mm².

Besides that, a rule concerning the scale effect for the plate thicknesses larger than 25mm were proposed. The investigations also showed a clear improvement of the fatigue resistance by the application of High Frequency Mechanical Impact Treatment (HFMI).

Detailed information on the small scale tests and results can be taken from [26].

5.6. Trough test program and execution

In order to investigate the complex stress state of thick-plate trough bridges considering the transversal bending effects, large scale trough bridge tests were planned, as realistically as possible. Therefore, drawings of existing thick-plate trough bridges have been provided by DB Netz AG and advisory project partners. The selected bridges have been evaluated in order to define the most relevant and thus realistic proportions of a typical thick-plate trough bridge. Consequently, the trough bridge specimens also reflected the residual stress state of such a real bridge.

In addition, the post-weld treatment method High Frequency Mechanical Impact (HFMI)

treatment has been applied in order to examine the possible improvement in view of fatigue strength for a real bridge structure.

The test program consisted of four small trough bridges, scaled from real bridges in a ratio of 1:3, with slight simplifications at the supports. As the test specimens were manufactured by four different steel construction companies, it was decided to apply HFMI-treatment only on one side of each test bridge to be able to compare the treated main girder to an untreated girder at the other side produced by the same fabricator.

The tests were executed at the Materials Testing Institute of the University of Stuttgart (MPA) with a portal frame on a testing field with two 1.000 kN hydraulic cylinders applying compression force with a stress ratio of $R = 0.1$.

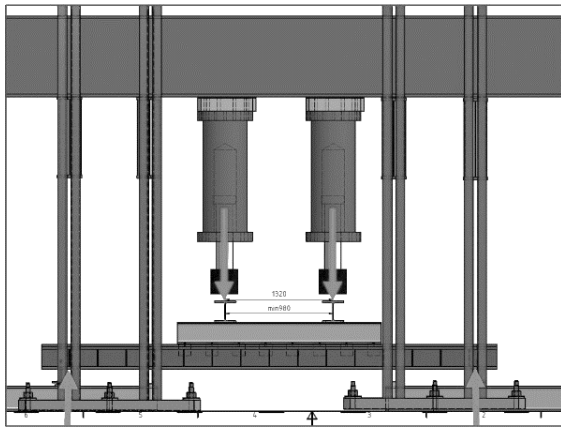


Fig. 17. Longitudinal view of test setup of trough tests.

In order to have realistic load behavior, the load introduction was realized with a downscaled ballast bed with typical railway gravel. Furthermore, downscaled railway sleepers and tracks were used to distribute the load of the two cylinders.

Fig. 17 shows the test-setup in the longitudinal view. Each test bridge was supported at four points. At all of these points the test bridge was enabled to move freely in plane. Hinged bearings were realized to avoid constraints, since the test setup defines the load introduction to be fixed points.

5.7. Results

The crack detection after and during the test was done with the help of the monitored strain gauges at chosen locations and with non-destructive testing such as fluorescent magnetic particle testing and dye penetration testing, where access

was possible. Since the inner side of the test bridge was filled with gravel for load distribution, it could be visualized only after the execution of the test.

The detected cracks mainly fell into two categories, the ones that led to global failure of the specimens and the ones that occurred, but were not dominant and did not harm the loading capacity of the whole test specimen.

With the help of strain gauges applied on the web, close to the fillet weld, and non-destructive crack testing it could be shown that the phenomenon of transversal bending of the web plates and welds exists. Especially at the inner side of the bridge on the longitudinal fillet welds, cracks appeared along the middle of the weld or at the weld toe in longitudinal direction, see Fig. 18. The location of these longitudinal cracks is mainly at the inner fillet weld, where the transverse stiffener and the web acts as a stiff T-section. It can be excluded that these cracks resulted of shear stresses, since they appeared at locations with low global shear stress. This is why those cracks seemed to be bending-induced. However, these cracks did not lead to a significant failure mode.

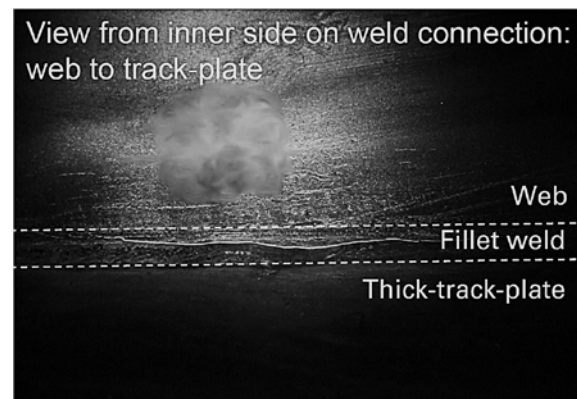


Fig. 18. Crack arising at inner side longitudinal weld of trough tests.

The failure cracks, which led to the global failure of the bridge were cracks rising across the longitudinal double fillet welds between the web and bottom flange. These cracks occurred in three of four cases at the untreated girder close to the stiffener, in the area of the girder where global shear and longitudinal stresses superimpose maximal, these points are marked with red circles in Fig. 19.



Fig. 19. Global location of failing cracks.

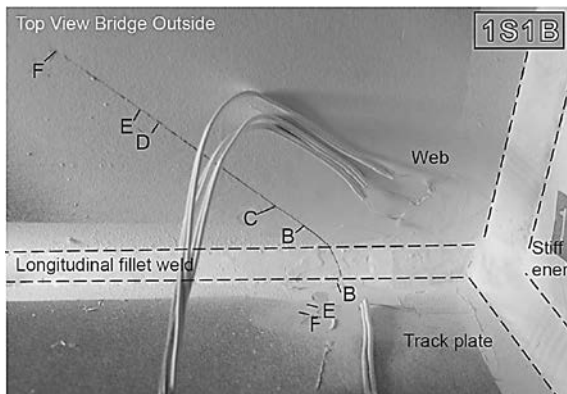


Fig. 20. Crack arising at outer side longitudinal weld of trough tests.

Cracks rising over the fillet weld (see Fig. 20) were usually dominant and led to the failure of the global structure. Fig. 20 illustrates the crack growth of such a main failure crack with different letters for the growing crack steps.

Due to the orientation and location of the crack and the relative premature failure it appears that there is a multi-axial effect. According to EN 1993-1-9 [1] only the direct stresses in the track plate should be considered when doing the fatigue check. Following the check on the detail

category 100, 112 or 125 depending on the welding requirements, it is expected to have a crack perpendicular to the fillet weld.

The results of the trough bridge tests, taking only the direct stresses of the track plate $\Delta\sigma_z$ into account, did not show consistent results. For none of the test specimens neither the 50 % line of the detail category 112 and 125 could be reached, nor the 95 % probability of survival, considering the total failure. Although 3 of 4 test specimens should theoretically be classified to detail category 112 and 125 due to the fact that the longitudinal welds were automatically welded.

Assuming that it might be not correct using only the direct stresses, but considering the principal stresses, as e.g. recommended in ECCS-Guideline [27], the evaluation results change. In the case of simultaneously occurring shear and direct stresses at the same location of a construction detail, [27] recommends to determine the highest principal stress and to use this as a basis for the fatigue verification. This approach correlates with the direction of the main failure crack as well as the results of the $S-N$ curve of the four trough bridge tests, see Fig. 21. The diagram in Fig. 21 shows the $S-N$ curve based on first principal stresses, which are illustrated at a sketch of an infinitesimal cut out. Finally, it may be concluded that in cases of simultaneously occurring stresses at one construction detail this recommendation should be followed, since the current approach of EN 1993-1-9 seems to be on the unsafe side.

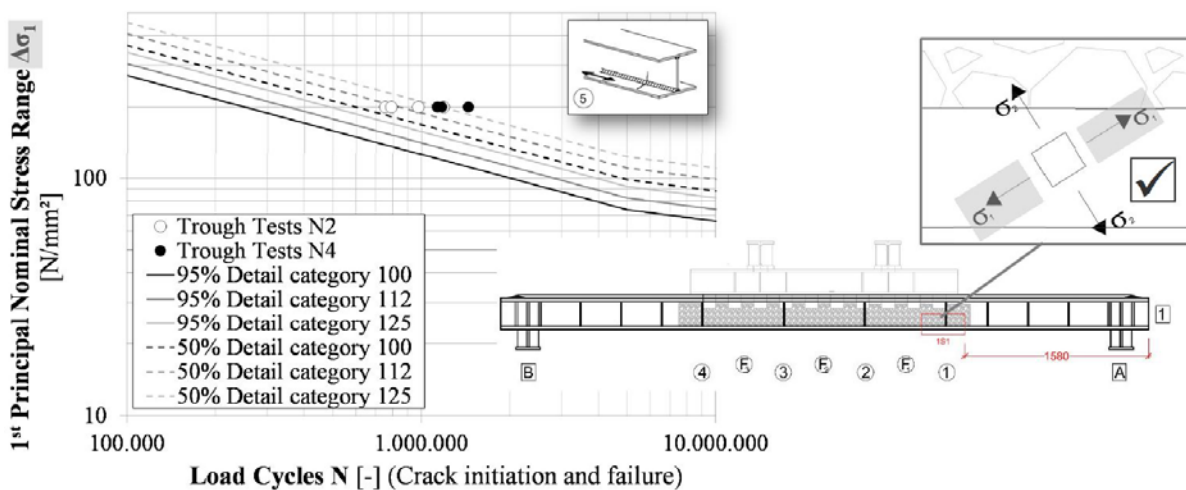


Fig. 21. Results in $S-N$ curve for tensioned continuous longitudinal welds [1] based on 1st principal stress ranges $\Delta\sigma_1$ [18].

In addition it should be mentioned that nearly in all cases the decisive crack started first and led to failure on the untreated girder. Therefore, one can say that the applied HFMI treatment for the trough bridge tests proved to be effective, for further information, see [28] and [18].

5.8. Summary

Within the small scale test series it could be shown that the fatigue resistance of a double fillet weld under transversal bending is less critical than expected and a detail category of 90 N/mm² was defined.

However, the small test series showed a significant size effect for the constructional detail of a double fillet weld under transversal bending, which should be considered.

The trough bridge tests with dimensions of a third of a real thick-plate trough bridge under realistic loading allowed an insight in the fatigue-caused failure mechanisms of this bridge type. Even though transversal bending led to cracks along the fillet welds, the main failure was caused due to the global longitudinal bending of the main girder.

However, the particularity of increased transversal bending of the thick plate and thus the cross section lead to a multiaxial stress state that should be considered for fatigue verification.

In addition, the effectiveness of HFMI treatment on always one of the two trough bridge test girders could be proved.

6. Fatigue strengths of welded uni- and multiplanar hollow section K-joints with thick-walled chords

6.1. Motivation

Over the last years steel-concrete composite highway bridges comprising 2D or 3D trusses made of thick-walled circular hollow sections (CHS) as shown in Fig. 1 (a) have become an innovative and aesthetic alternative to the conventional bridges in Europe. The so-called K-joint is a major constructional detail of 2D trusses normally consisting of rising and falling, but not crossing braces and a continuous bottom chord forming together a lying ‘K’ at the intersection. In terms of 3D trusses, KK-joints are the intersections of two brace planes. From the viewpoint of economics and ease of construction the braces

are preferred being welded directly onto the bottom chord. This is due to the fact that directly welded hollow section joints avoid the use of cost-intensive cast steel nodes and therefore, the fragmentation and the butt welding of the highly stressed chords.

For this type of hollow section joints the nominal stress approach can only be applied in cases, where the wall-thicknesses do not exceed values of 8 mm and where the nominal stresses at the weld toes can be determined. If the nominal stress approach cannot be applied, the structural stress or hot-spot stress approach gives a powerful alternative of fatigue design. However, this design approach is limited for CHS joints by the design rules of CIDECT [5] and DNV [6] to $\gamma = d_0 / (2 \cdot t_0) \geq 12$ and 8 respectively. This can be attributed to a lack of a statistically appropriate number of test results within the existing test database. Recently, more and more welded thick-walled tubular K-joints with low chord slenderness $\gamma < 12$ have been realized. Therefore, a proposal for the fatigue strength (finite fatigue life regime, as-welded, in air) of uni- and multiplanar welded CHS K-joints with chord slenderness values between $3 \leq \gamma \leq 12$ has been derived in a recently finalized German research project [3].

In this paper, the chord of a K-joint is considered as absolutely thick-walled if its wall thickness t_0 exceeds the reference wall thickness $t_{ref} = 16$ mm of the CIDECT detail category, for which no size effect has to be considered, see also Table 2. With respect to the limitation of the CIDECT design recommendations, the chord of a K-joint with $\gamma < 12$ is referred to as relatively thick-walled, also Table 2.

Table 2. Definition of hollow-section wall-thickness, taken from [29].

Wall thickness	thick-walled	thin-walled
absolute	$t_0 > t_{ref}$	$t_0 \leq t_{ref}$
relative, $\gamma = d_0 / (2t_0)$	$\gamma < 12$	$\gamma \geq 12$

Illustration

6.2. State of the art

6.2.1. Structural stress approach

The joints of 2D or 3D trusses made of circular hollow sections, including K-joints, represent areas of high stress concentrations. This is on one hand due to the fact that in these areas an

increase of stiffness occurs caused by the overall cross-sectional change. On the other hand, the welds lead to an additional undefined stress increase as a result of their residual stresses, local notch effects and material inhomogeneities, induced by the welding processes. Therefore, the determination of real stresses is difficult or even impossible. However, the determination of so-called hot-spot or structural stresses is feasible also for practitioners. The structural stress approach does only focus on the local weld-notch on a „micro-base“ (i.e. the fillet or butt weld) and not on the specific material welding influences nor on the constructional detail in general, as for example the whole K-joint.

6.2.2. Determination of structural stresses

In general, structural stresses can be determined either by numerical calculations or by measurements. For the calculation of structural stresses using a finite element analysis, the real structure has to be converted into a numerical model and discretized into an appropriate amount of small finite elements. Afterwards, the stresses perpendicular to the weld toe (according to the recommendations in [5]) are determined with a linear-elastic calculation at two or three positions at defined distances. Finally and according for example to [5], the structural stresses can be identified by extrapolating the calculated stresses to the weld toe, see Fig. 22.

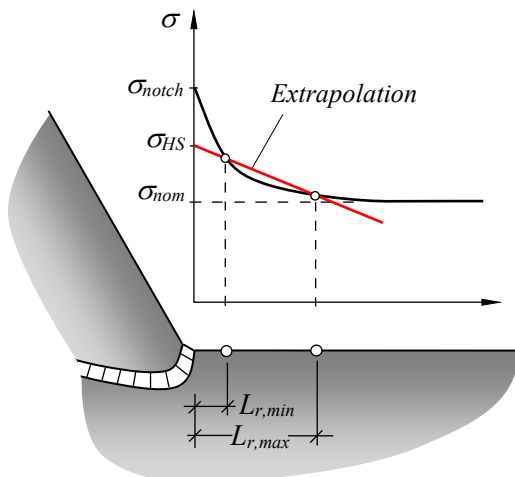


Fig. 22. Determination of structural stresses σ_{HS} at the crown toe of a circular hollow section joint, taken from [3].

In this context, it is necessary to fulfill the requirements related to the FE-model and the FE-meshing, which can also be found in the literature, see [30]. Also, it should be noted that structural stresses are only theoretical or rather fictional stresses, which cannot be found in real

structures and which vary in a circumferential manner around the braces. Due to the efforts needed and the need of validation, this method is still an exception in practice.

However, the use of so-called *SCF*-values (Stress Concentration Factors) is possible and more common in practice. These values have been developed through extensive numerical parameter studies and were verified by experimental data. In this case, the structural stresses can be calculated from the nominal stresses, which have been determined with a linear elastic calculation on the overall system, by a simple multiplication with the *SCF*-values, see Eq. (5).

$$\Delta\sigma_{HS} = SCF \cdot \Delta\sigma_{nom} \quad (5)$$

Two of the most commonly used tables to define *SCF*-values for tubular structures are those from CIDECT [2] and *Efthymiou* [31]. Recently, several research projects were conducted focusing on the extension of the already existing *SCF*-values under consideration of multiple load cases and geometrical configurations, like the investigations of *Schumacher* [32] or the German research project conducted at the University of Stuttgart and financed by the German Federal Highway Research Institute (BAST) [33].

6.2.3. Fatigue strength based on structural stresses

The fatigue strength of a tubular joint can be described by Eq. (6). The fatigue strength depends on a particular number of cycles N , for which the fatigue strength has to be evaluated, normally for the detail category $\Delta\sigma_C$ two million stress cycles and the value m of the S - N curve. Eq. (6) also includes a term for the consideration of the size effect.

$$\Delta\sigma_R = \underbrace{\Delta\sigma_C}_{\text{detail category}} \cdot \underbrace{\left(\frac{t_{ref}}{t}\right)^B}_{\text{size effect}} \quad (6)$$

According to *Ørjasæter* [34] the size effect describes the influence of wall-thickness of welded components on their fatigue strengths. It can be divided into a statistical, geometrical and technological size effect. As this effect can be observed for thick-walled tubular trusses, it is considered in Eq. (6) by a term which includes a reference wall thickness t_{ref} and a corresponding exponent B , both set by the various standards. It stands out, that the term for the consideration of the size effect is nearly the same as for lamellae

joints, given in Eq. (4). In contrast, the reference wall-thickness is given in [1] as $t_{ref} = 25$ mm. Additionally, the correction factor is denoted as n and not B as in Eq. (6). An overview of the derived detail categories and assumed parameters of different common fatigue design recommendations is given in Table 3. In all cases, the value m of the $S-N$ curve is fixed to 3.

Table 3. Fatigue strength (structural stresses) in selected design recommendations. Extracted from [3].

	EC3	DNV	API	CIDECT
$\Delta\sigma_c$ [MPa] (air)	114 ^a	90 ^b	114 ^c	114
Survival probability [%]	95 ^a	97.7	97 ^c	95
Failure criterion	through-crack ^e	through-crack	through-crack ^c	through-crack ^d
Ref. wall thickness t_{ref} [mm]	16 ^a	32	16	16
Exponent B of size effect	–	0.25	0.25	0.06 log N
Positive effect for $t < t_{ref}$?	–	no	no	yes

^a following van Wingerde *et al.* [35], p. 126 & 133
^b curve T [6]
^c API RP 2A-WSD [36], Sec. C5.2.5 & p. 58, 214
^d Zhao & Packer [5], p. 5
^e following [5]

As the above mentioned design recommendations cover only slender K-joint geometries, there had been doubts if these derived fatigue

strengths can also be recommended for tubular K-joints whose geometries lie below the above mentioned range. To answer this question by experimental evidence, a research project [3] was set up aiming to fill the gap of knowledge concerning the fatigue behavior of thick-walled welded K-joints and to enlarge the application range of this type of constructional detail, see sec. 6.3.

6.3. Experimental Investigations

The research project [3] comprised a comprehensive test program and detailed numerical investigations. It was carried out by four partners: (i) University of Stuttgart, (ii) Munich University of Applied Sciences, (iii) Munich University of Armed Forces and (iv) Schweisstechnische Lehr- und Versuchsanstalt (SLV) Halle. In General, the test program included more than 80 single-joint fatigue tests on 2D and 3D CHS K-joints as well as one fatigue test on a large-scale girder spanning about 11 m in order to examine the transferability of the test results from the single joint tests to large-scale structures. Of these tests, 61 were performed at an as-welded condition and are addressed in Table 4. The remaining 20 single-joint fatigue tests investigated the influence of a post-weld treatment on the fatigue strength and are not covered in this paper. The single joint fatigue tests on CHS K- and KK-joints with thick-walled chords ($\gamma < 12$) were in-

Table 4. Overview of test series in Kuhlmann *et al.* [3].

Symbol	Series	Loading ^a	R	Joint	Chord	Brace	γ	No.
◇	1	Chord – IPB	> 0	K	177.8 × 20	88.9 × 5	4.45	5
○	1	Chord – AX	> 0	K	177.8 × 20	88.9 × 5	4.45	2
▽	1	Brace – IPB	– 1	K	177.8 × 20	88.9 × 5	4.45	3
□	1	Brace – AX	– 1	K	177.8 × 20	88.9 × 5	4.45	9
◇	2	Chord – IPB	> 0	K	177.8 × 20	88.9 × 12.5	4.45	5
○	2	Chord – AX	> 0	K	177.8 × 20	88.9 × 12.5	4.45	2
▽	2	Brace – IPB	– 1	K	177.8 × 20	88.9 × 12.5	4.45	2
□	2	Brace – AX	– 1	K	177.8 × 20	88.9 × 12.5	4.45	8
✦	3	Chord – IPB	> 0	K	273.0 × 40	139.7 × 10	3.41	5
✦	4	Chord – IPB	> 0	K	273.0 × 40	139.7 × 16	3.41	4
⊗	4	Chord – IPB	– 1	K	508.0 × 40	244.5 × 25	6.35	2
⊗	4	Chord – IPB	– 1	K	508.0 × 60	244.5 × 25	4.23	2
⊕	5	Chord – IPB	– 1	K	273.0 × 40	139.7 × 10	3.41	2
☆	6	Chord – IPB	> 0	KK	177.8 × 20	88.9 × 5	4.45	3
☆	6	Chord – AX	> 0	KK	177.8 × 20	88.9 × 5	4.45	1
★	8	Combined	– 1	K	177.8 × 20	88.9 × 5	4.45	2
★	8	Combined	– 1	K	177.8 × 20	88.9 × 12.5	4.45	2
●	Girder	Combined	0.1	K	193.7 × 25	88.9 × 12.5	3.87	–
▼	Girder	Combined	0.1	KK	193.7 × 25	88.9 × 12.5	3.87	–

^a IPB: in-plane bending; AX: axial force

investigated at four elementary load cases as depicted in Fig. 23. All these tests were carried out with a constant stress amplitude.

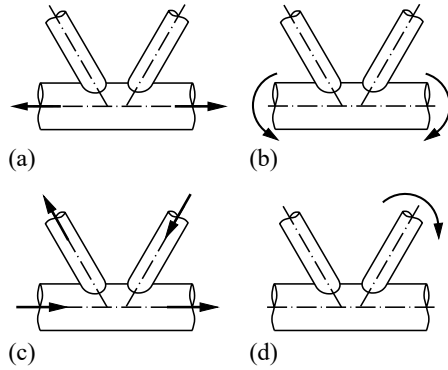


Fig. 23. Investigated elementary loading cases: (a) chord axial force, (b) chord bending, (c) brace axial force, (d) brace bending, taken from [3].

The chords had diameters from 177.8 to 508.0 mm with wall thicknesses of 20 to 60 mm. The braces had diameters of 88.9 to 244.5 mm with wall thicknesses of 5 to 25 mm. The braces of all test specimens of the single joint fatigue tests had an angle of 60°. The tests with brace axial force and brace bending were carried out at the Materials Testing Institute (MPA) of the University of Stuttgart on behalf of the Institute of Structural Design. Among these, the tests with brace axial force were conducted on a special test rig, consisting of three hydraulic jacks working synchronously at a stress ratio of $R = -1$ and a frequency of 0.5 to 1.3 Hz, see Fig. 24. In all cases, the first through-wall-thickness crack was set as failure criterion.

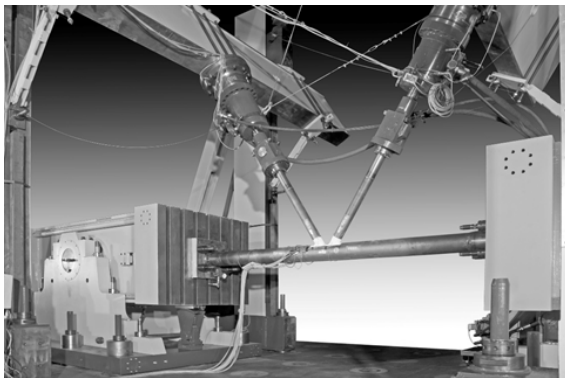


Fig. 24. Test rig for testing under brace axial force and combined loading at the Materials Testing Institute (MPA) of the University of Stuttgart, Germany, from [3].

6.4. Test results

The results of all conducted tests of Kuhlmann *et al.* [3] are visualized in Fig. 25. As

the fatigue tests had to be performed with different stress ratios R , due to technical reasons and the failing wall thickness varied depending on the load case, the depicted test data in Fig. 25 have been modified accordingly.

In [3] it had been concluded that for all as-welded test specimens the cracks were initiated at the weld toes of either the chord or the brace. For the load cases “chord axial force” and “chord bending”, the decisive through-thickness cracks were exclusively initiated at the weld toes of the chord either at the crown toe or at the crown heel. Under “brace axial force” the first through-cracks were detected in the gap region. Depending on the wall-thickness ratio, $\tau = t_1/t_0$, the through-wall-thickness crack occurred in the brace (for $\tau = 0.25$) or the chord wall (for $\tau = 0.63$). For the load case “brace bending” with a stress ratio $R = -1$, cracks initiated at several locations, either in the chord or the brace.

6.5. Numerical investigations

In addition to the conducted fatigue tests, a numerical analysis was performed in order to determine the arising structural stress amplitudes within the test specimens. A 3D-parameterized Finite Element (FE) model made up of 20-node solid elements was generated with ANSYS 14.0. Subsequently, the model was validated through strain measurements recorded in preliminary static tests. The structural stresses were then calculated as described in Section 6.2.2. As already mentioned, the test program involved tests conducted with different stress ratios R , including tests with alternating loads ($R = -1$). In order to account for the positive effect of “crack-closing” compressive stresses, the mean stress effect with moderate residual stresses was assumed. The calculated fatigue strengths were then modified by using Eq. (7) derived from EN 1993-1-9 [1], Sec. 7.2.1.

$$\Delta\sigma_{HS}^{R=0} = \frac{\Delta\sigma_{HS}^{R=-1}}{1.125} \quad (7)$$

In addition and for reasons of comparability, the size effect was taken into account by modifying the stress ranges with Eq. (6), where the reference wall thickness t_{ref} and the exponent B were chosen according to the recommendations of CIDECT [5], see also Table 3.

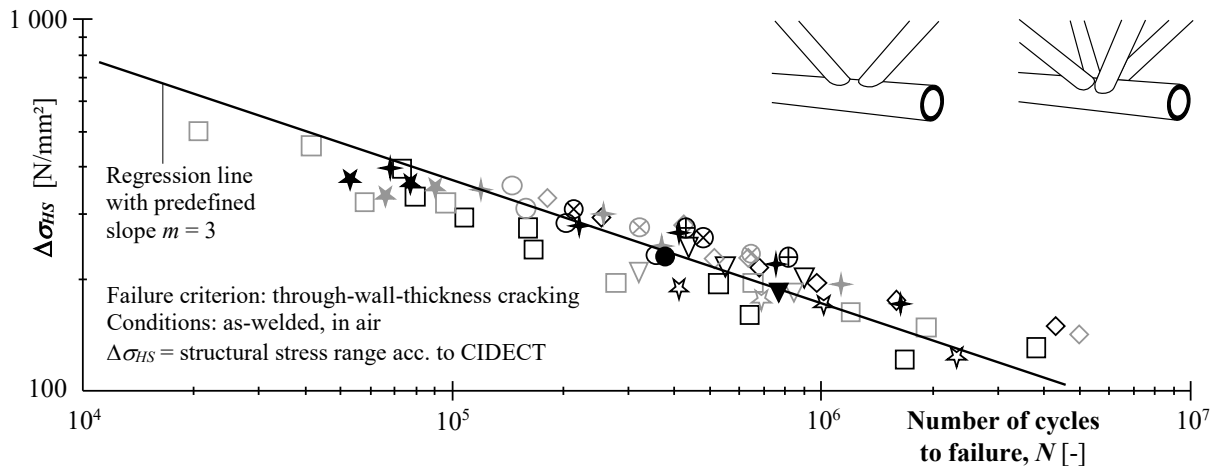


Fig. 25. Test data of Kuhlmann *et al.* [28] modified for failing wall thickness and stress ratio R (for symbols see Table 4).

6.6. Statistical evaluation

For the statistical evaluation of CHS K- and KK-joints in the as-welded condition, the results of 59 single joint fatigue tests could be used, included in Fig. 25. The outcome of the statistical evaluation for the failure criterion of the first through-wall-thickness crack is summarized in Table 5.

Table 5. Characteristic reference value $\Delta\sigma_C$ [N/mm²] of fatigue strength (structural stresses) for 2 million stress cycles and reference wall thickness 16 mm; failure criterion: through-wall-thickness cracking; conditions: as-welded, in air; survival probability according to Eurocode 3, extracted from [29].

Scope	S-N curve		Ref.	No.
	$m = 3$	$m = \text{var.}$		
K/KK joints $\gamma < 12$	104	116	‡	59
Tubular joints $\gamma \geq 12$	107	–	*	115

‡ = Kuhlmann *et al.* [3]
* = van Wingerde *et al.* [35], p. 133

It can be observed, that the fatigue strength of the investigated CHS K- and KK-joints with thick-walled chords of $\Delta\sigma_C = 104$ N/mm² corresponds quite well with that for thin-walled tubular joints of $\Delta\sigma_C = 107$ N/mm², given in [35] and Table 5 for a fixed value of $m = 3$.

6.7. Summary

Through experimental evidence it has been shown that the fatigue strength of $\Delta\sigma_C = 104$ N/mm² (finite life regime, as-welded,

in air, criterion: through-wall-thickness cracking) of uni- and multiplanar welded CHS K-joints with thick-walled chords ($3 \leq \gamma \leq 12$) is comparable to that of tubular joints covered by the existing CIDECT detail category. For the tested specimens the size effect depended primarily on the failing wall thickness. The influence of the chord slenderness γ was not significant.

All investigated K- and KK-joints were planned and fabricated with a brace angle of 60°, which is why varying brace angles were investigated in the accompanying numerical analysis. It could be concluded, that the determined fatigue strengths can also be recommended for differing brace angles.

The results of the girder fatigue test have shown that the fatigue strengths determined in the single joint tests can also be recommended for whole large scale structures. In this case, the test was carried out with a variable stress amplitude, in order to determine the through-wall-thickness cracks by considering the occurring beach marks. Subsequently the fatigue strengths could be successfully derived by using the Palmgren-Miner rule.

With all conducted fatigue tests and the accompanying numerical analysis, the successful application of the proportional size effect according to the CIDECT design rules [5] could be shown. Therefore, the size effect according to [5] can be recommended for thick-walled K- and KK-joints within the investigated geometry range.

6.8. Outlook

When investigating the weld surfaces and roots of the tested and welded CHS joints, irregularities could be identified in the weld, which had not led to the decisive through-crack. Therefore, a certain amount of “allowable” irregularities seem to be possible. However, a reliable detection of internal weld irregularities by non-destructive testing (NDP) is needed. Hence, in order to increase the acceptance of directly welded CHS joints it is important to investigate and quantify the influence of weld irregularities, such as incomplete fusions and weld root openings, on the fatigue strength and to further develop the methods to detect them. These aspects are addressed in a further still running German research project (*Kuhlmann et al.* [37]).

Another aspect addressed within this project, is the transferability of the test results from the single joint tests in [3] to structures with chord diameters larger than 508 mm, especially in order to create the transition to typical dimensions of offshore structures.

7. Conclusions

In this paper three different constructional details and the outcome of four different research projects, conducted by the Institute of Structural Design of the University of Stuttgart have been presented. The projects are: No. P815 [3] and No. P978 [18] of the Research Association for Steel Application (FOSTA) as well as Project No. 15380 [15] and No. 17104 [16] of the German Committee for Steel Construction (DAST). These projects had the aim, to investigate constructional steel bridge details which are not fully covered by the currently existing design rules and to extend the application range of Eurocode 3 Part 1-9 [1].

In [18] it could be concluded, that the fatigue resistance of a double fillet weld under transversal bending is less critical than expected. Even though transversal bending leads to cracks along the fillet welds, the main failure is caused by the global longitudinal bending of the main girder. Finally, it has been recommended, that the particularity of increased transversal bending for the thick plate and thus the cross section leads to a multiaxial stress state that should be considered also for fatigue design using principal stresses for the nominal stress approach.

Due to the highly stressed joint region the use of the structural stress approach proved to be

most appropriate for welded joints of round hollow sections. In [3] it could be shown, that the fatigue strength of uni- and multiplanar welded CHS K-joints with thick-walled chords ($3 \leq \gamma \leq 12$) is comparable to that of thin-walled tubular joints covered by the existing CIDECT detail category. For the tested specimens the size effect depended primarily on the failing wall thickness. The influence of the chord slenderness γ was not significant.

In both, [18] and [3] it was concluded that the results of the small scale fatigue tests can be transferred to large scale structures. Hence, the derived fatigue strengths can be recommended for structures with larger and real dimensions respectively.

With all conducted fatigue tests (in [18], [3], [15] and [16]) a significant influence of the size effect was confirmed. In [3] the successful application of the proportional size effect according to the CIDECT design rules [5] was shown. Therefore, the size effect according to [5] can be recommended for thick-walled K- and KK-joints within the investigated geometry range. In [16] a pronounced size effect was detected for the lamellae joints considering the overall thickness. A size effect, according to [1], Tab. 8.3 can be recommended. Also in [18] a size effect for the transversal bending of double fillet welds could be observed.

All these investigations establish the possibility of the extension of the Eurocode 3 Part 1-9, in order to update the existing detail catalogue and to include constructional details being important for today’s bridge design.

First steps in the direction of an adoption of the here presented constructional details, as the lamellae joint (Chapter 4), the double fillet weld under transversal bending (Chapter 5) or the thick-walled circular hollow section K-joint (Chapter 6) into the Eurocode 3 Part 1-9 were made by discussions in the responsible Working Group CEN TC250/SC3/WG9.

8. Acknowledgements

The work presented is carried out as part of several joint research projects (P815 [3], P978 [18]) of the Research Association for Steel Application (FOSTA) and (No. 15380 [15], No. 17104 [16]) of the German Committee for Steel Construction (DAST). They were financed over

the AiF within the development program for industrial community research and development (IGF) from the Federal Ministry of Economic Affairs and Energy (BMWi) based on a decision of the German Bundestag.

The research project [18] was a joint project with colleagues from University of Stuttgart (Institute of Structural Design and Department of Life-Cycle Engineering), Technical University of Munich, and Karlsruhe Institute of Technology.

The research project [3] was carried out by four partners: (i) University of Stuttgart, (ii) Munich University of Applied Sciences, (iii) Munich University of Armed Forces and (iv) Schweisstchnische Lehr- und Versuchsanstalt (SLV) Halle.

The authors thank for their cooperation.

In addition, the authors want to take this opportunity to express their profound gratitude to all supporters of their research. We thank DB Netz AG for their provision of data and knowledge, AG der Dillinger Hüttenwerke for provision of materials, DONGES Steeltec GmbH, MCE GmbH, SEH Engineering and Stahlbau Magdeburg for donation of the fabrication of specimens and Max Bögl Stahl- und Anlagenbau GmbH & CoKG for short-term help with the fabrication. Special thank goes to PITec GmbH for the treatment of specimens and Consulting Office Meyer+Schubart for advisory support. Further special thanks goes to Vallourec Deutschland GmbH for the donation of more than 50 tons of circular hollow sections and to ZIS Industrietechnik GmbH, Meerane for the donation of the pre-cut of the CHS.

Moreover, the authors would like to thank all project partners for their good and fruitful cooperation.

References

- [1] EN 1993-1-9: 2005 + AC: 2009. Eurocode 3: Design of steel structures – Part 1-9: Fatigue; 2009.
- [2] EN 1993-2: 2006 + AC:2009. Eurocode 3: Design of steel structures – Part 2: Steel Bridges; 2009.
- [3] Kuhlmann U, Bucak Ö, Mangerig I, Kranz B, Euler M, Hubmann M, Fischl A, Hess A, Hermann J, Zschech R. FOSTA P815 - Fatigue-resistant trusses of circular hollow sections with thick-walled chords (in German). Düsseldorf: FOSTA Forschungsvereinigung Stahlanwendung e. V.; 2014.
- [4] Hobbacher A. Recommendations for fatigue design of welded joints and components, IIW-Documents No. XIII-2151-07 / XV-1254-07. 2007.
- [5] Zhao XL, Packer JA. Recommended Fatigue Design Procedure for Welded Hollow Section Joints, IIWDoc. XIII-1772-99/XV-1021-99;1999.
- [6] DNV-RP-C203: 2010. Fatigue design of offshore steel structures – Recommended practice. Det Norske Veritas; 2010.
- [7] Kuhlmann U, Schmidt-Rasche C. Next Generation of Eurocode 3 – Evolution by improvements and harmonization. Conference proceedings of XI. Conference on Steel and Composite Construction. Coimbra; 2017.
- [8] CEN TC 250 N993, Response to Mandate M/515 (Mandate for amending existing Eurocodes and extending the scope of structural Eurocodes) ‘Towards a second generation of EN Eurocodes’, Brussels; May 2013.
- [9] Drebenstedt K, Euler M. Statistical Analysis of Fatigue Data according to Eurocode 3. Conference proceedings of 9th International conference on bridge maintenance, safety and management (IABMAS). Melbourne; 2018. [in preparation]
- [10] Basquin OH. The exponential law of endurance tests. American Society for Testing and Materials Proceedings, Vol 10: 625-630; 1910.
- [11] EN 1990: 2002 + A1: 2005 + A1: 2005/AC: 2010. Eurocode 0: Basis of structural design. Annex D, D.8: Statistical determination of resistance models; 2010.
- [12] Wadsworth HM. Handbook of statistical methods for engineers and scientists, 2nd ed., New York: Mcgraw-Hill; 1998.
- [13] DS 804: Vorschrift für Eisenbahnbrücken und sonstige Ingenieurbauwerke. Druckschriftenwerk der Deutschen Bahn AG; 2000.
- [14] TGL 16500/01: Stahlbau – Stahltragwerke. Grundlagen der Berechnung nach Grenzzuständen mit Teilsicherheitsfaktoren, Bauliche Durchbildung; 1988.
- [15] Kuhlmann U, Euler M, Kudla K. Weiterentwicklung und Spezifizierung der Ermüdungsnachweise im Stahl- und Verbundbrückenbau. Final report of research project DAST/IGF No. 15380 N/1; 2011.
- [16] Kuhlmann U, Kudla K. Ermüdungsfestigkeit von Montagestößen in Vollwandträgern mit dicken Gurten. Final report of research project DAST/IGF No. 17104; 2015.
- [17] Kuhlmann U, Kudla K. Ermüdungsfestigkeit von Lamellenstößen bei Vollwandträgern mit dicken Gurten, Experimentelle und numerische Untersuchungen. Stahlbau 2015;84(3):203-212.
- [18] Kuhlmann U, Breunig S, Pascual AM, Maier P, Ummenhofer T, Zinke T, Mensinger M,

- Pfaffinger M, Beck T, Lenz K, Schneider S. Ganzheitliche Bewertung von Stahl- und Verbundeisenbahnbrücken nach Kriterien der Nachhaltigkeit. Final report of research project P978, NaBrueEis. Düsseldorf: FOSTA Forschungsvereinigung Stahlanwendung e. V.; 2016.
- [19] Zinke T, Ummenhofer T, Lenz K, Schneider S, Beck T. Operational, Ecological and Economical Assessment of Steel Railway Bridges. Eurosteel-Proceedings; 2017.
- [20] Breunig S. Bewertung der Ermüdungsfestigkeit von Schweißnähten und ihrer Nachbehandlung im Brückenbau. Dissertation, in progress; 2019.
- [21] EN 1991-2: 2003 + AC: 2010. Eurocode 1: Actions on structures – Part 2: Traffic loads on bridges; 2010.
- [22] Schrade C. Ermüdungsprobleme prismatischer, trogförmiger Eisenbahnbrücken mit dicken Trogblechen und deren Bewältigung. Stahlbau 2010;79:136 – 143.
- [23] Schardt R. Verallgemeinerte Technische Biegetheorie. Band 1 – Lineare Probleme. 2. Edition. Darmstadt: Metrum-Verlag; 2008.
- [24] Günther HP. Ermüdungsverhalten von Stahlträgern mit schlanken Stegblechen im Brückenbau. Dissertation, Institut für Konstruktion und Entwurf, Universität Stuttgart, Mitteilung No. 2002-1; 2002.
- [25] Kuhlmann U, Euler M. Kranbahnträger – Wirtschaftliche Bemessung und Konstruktion robuster Radlasteinleitungen. Final report of research project DAST/AiF-Nr. 14173; 2007.
- [26] Breunig S, Kuhlmann U. Improvement of Fatigue Resistance of Transversally Bended Longitudinal Fillet Welds by High Frequency Mechanical Impact Treatment. Proceedings of the International Symposium on Steel Bridges; 2015.
- [27] Recommendations for the fatigue design of steel structures, ECCS – Technical Committee 6 – Fatigue, ECCS-Publication No. 34; 1985.
- [28] Breunig S, Kuhlmann U. Experimental Tests on the Fatigue Behaviour of Thick-Plate Trough Railway Bridges, Eurosteel Proceedings; 2017.
- [29] Euler M, Bove S, Kuhlmann U. Fatigue-resistant trusses of circular hollow sections with thick-walled chords. European Steel Technology and Application Days. 2015. METEC & 2nd ES-TAD. Düsseldorf, 15 - 19 June 2015.
- [30] Niemi E, Fricke W, Maddox SJ. Structural Hot-Spot Stress Approach to Fatigue Analysis of Welded Components. Designer's Guide. Second Edition. Springer. Finland, Germany, UK; 2018.
- [31] Efthymiou M, Durkin S. Development of SCF formulae and generalized influence functions for use in fatigue analysis. In: Proceedings of the Conference on Recent Developments in Tubular Joints Technology. Surrey, UK; 1988.
- [32] Schumacher A. Fatigue behaviour of welded circular hollow section joints in bridges. PhD Thesis, École Polytechnique Fédérale de Lausanne (EPFL), Switzerland; 2003.
- [33] Kuhlmann U, Euler M. Recommendations for welded KK-joints in road bridge construction (in German). Berichte der Bundesanstalt für Straßenwesen. Heft B 71. Bergisch Gladbach; 2010.
- [34] Ørjasæter O. Effect of plate thickness on fatigue of welded components (IIW-Doc. JWG XIII-XV-118-93); 1995.
- [35] van Wingerde AM, van Delft DR, Wardenier J, Packer JA. Scale effect on the fatigue behavior of tubular structures. In Maddox, S. J. & Prager, M. (ed.), Proc. of the International Conference on Performance of Dynamically Loaded Welded Structures, IIW 50th Annual Assembly Conference, San Francisco, 14-15 July 1997: 123-135; 1997.
- [36] API RP 2A-WSD. Recommended practice for planning, designing and constructing fixed offshore platforms – working stress design. American Petroleum Institute (API); 2005.
- [37] Kuhlmann U, Dürr A, Steinhausen R, Bove S, Roth J, Pientschke C. FOSTA P1163 - Economical design of welded circular hollow section joints under fatigue loading in consideration of the required weld quality (in German). In process; 2018.